Quasistationary distributions for the Domany-Kinzel stochastic cellular automaton

A. P. F. Atman* and Ronald Dickman†
Departamento de Fìsica, Instituto de Ciências Exatas, Universidade Federal de Minas Gerais, C. P. 702 30123-970, Belo Horizonte, MG, Brazil

(Received 10 July 2002; published 28 October 2002)

We construct the *quasistationary* (QS) probability distribution for the Domany-Kinzel stochastic cellular automaton (DKCA), a discrete-time Markov process with an absorbing state. QS distributions are derived at both the one-and two-site levels. We characterize the distributions by their mean, and various moment ratios, and analyze the lifetime of the QS state, and the relaxation time to attain this state. Of particular interest are the scaling properties of the QS state along the critical line separating the active and absorbing phases. These exhibit a high degree of similarity to the contact process and the Malthus-Verhulst process (the closest continuous-time analogs of the DKCA), which extends to the scaling form of the QS distribution.

DOI: 10.1103/PhysRevE.66.046135 PACS number(s): 05.10.Gg, 02.50.Ga, 05.70.Ln, 05.40.−a

I. INTRODUCTION

The Domany-Kinzel stochastic cellular automaton (DKCA) [1] is a Markov process that exhibits a phase transition from an active state to an absorbing one. Stochastic processes with an absorbing state arise frequently in statistical physics [2], and are currently of great interest in connection with self-organized criticality [3] and nonequilibrium critical phenomena [4,5]. Many studies of the DKCA and related probabilistic cellular automata (PCA) have been published, using deterministic mean-field equations [6–8], Monte Carlo simulations [9–13] and renormalization group (RG) analyses [14–16].

While the mean-field (MF) description of the DKCA admits (for appropriate parameter values) an active stationary state, for finite system sizes the model always ends up in the absorbing state, due to fluctuations. MF theories ignore such fluctuations, and so are incapable of treating finite systems. But, since simulations and other numerical methods typically study finite systems, it is of interest to develop approximate theoretical descriptions that account for finite system size. A natural way to study finite systems with an absorbing state is via the *quasistationary distribution*, which, when it exists, describes the asymptotic properties conditioned on survival [17–19]. Recently, mean-field-like methods were developed for studying the quasistationary state of finite systems with an absorbing state [20]. The quasistationary properties converge to the true stationary properties in the infinite-size limit. (Indeed, this provides the rationale for studying the ''stationary'' behavior of absorbing-state models in simulations, which of necessity treat finite systems.) In Ref. [20], quasistationary distributions for various continuous-time Markov processes are constructed, in particular, for the contact process (CP) and the closely related Malthus-Verhulst process (MVP). In the case of the CP, both one-and two-site approximations are derived. In this work, we extend the analysis to *discrete-time* processes, using the DKCA as an interesting example, closely related to the CP.

The remainder of this paper is structured as follows. In Sec. II we review the one-and two-site MF approximations for the DKCA. In Sec. III, we construct the quasistationary (QS) probability distribution at the site level. The QS distribution at the pair level is discussed in Sec. IV, while Sec. V presents our conclusions.

II. SITE AND PAIR MF APPROXIMATIONS

In this section we review the definition of the DKCA and its mean-field description at the one-and two-site levels [6,8]. The DKCA is a discrete-time Markov process (all sites are updated simultaneously), whose configuration is given by a set of stochastic variables $\{\sigma_i\}$ ($\sigma_i=0$ or 1), defined at sites i and times $t=0,1,2,\ldots$, such that $t+i$ is even. Let σ represent the configuration at time t, and $P_t(\sigma)$ the probability distribution in configuration space. The evolution of the latter is governed by [22]

$$P_{t+1}(\sigma)=\sum_{\sigma'}\ \omega(\sigma|\sigma')P_t(\sigma'), \tag{1}$$

where $\omega(\sigma|\sigma')$ denotes the probability of the transition $\sigma' \to \sigma$, and enjoys the properties $\omega(\sigma|\sigma')\geqslant 0$ and $\Sigma_\sigma \omega(\sigma|\sigma')=1$. The transition probability for the DKCA is a product of factors associated with each site:

$$\omega(\sigma|\sigma')=\prod_{i=1}^{L}\ w_i(\sigma_i|\sigma'), \tag{2}$$

where $w_i(\sigma_i|\sigma')$ is the conditional probability for site i to be in state σ_i at time $t+1$, given configuration σ' at time t. The probabilities $w_i(\sigma_i|\sigma')$ are translation-invariant and in fact depend only on the variables σ'_{i-1} and σ'_{i+1} at the previous time step:

$$w_i(\sigma_i|\sigma')=w_{DK}(\sigma_i|\sigma'_{i-1},\sigma'_{i+1}). \tag{3}$$

The above relations, with the transition probabilities given in Table I, define the DKCA. Noting that the transition (00) $\to(1)$ is prohibited, we see that the configuration $\sigma_i=0$, $\forall i$ is *absorbing*.

*Email address: atman@fisica.ufmg.br
†Email address: dickman@fisica.ufmg.br

 ©2002 The American Physical Society

TABLE I. DKCA transition probabilities.

$\sigma_i \vert \sigma'_{i-1}, \sigma'_{i+1}$	1,1	1,0	0,1	0,0
1	p_2	p_1	p_1	0
0	$1-p_2$	$1-p_1$	$1-p_1$	1

Of interest are the n-site marginal probabilities. The evolution of the one-site distribution $P_t(\sigma_i) \equiv \Sigma_{\sigma_j, j\neq i} P_t(\sigma)$, is given by

$$P_{t+1}(\sigma_i) = \sum_{\sigma'_{i-1}} \sum_{\sigma'_{i+1}} w_{DK}(\sigma_i \vert \sigma'_{i-1}, \sigma'_{i+1}) P_t(\sigma'_{i-1}, \sigma'_{i+1}), \tag{4}$$

where $P_t(\sigma'_{i-1}, \sigma'_{i+1})$ is the marginal distribution for a pair of nearest-neighbor sites. The evolution of the latter is coupled to the three-site probability, so

$$P_{t+1}(\sigma_{i-1}, \sigma_{i+1}) = \sum_{\sigma'_{i-2}} \sum_{\sigma'_i} \sum_{\sigma'_{i+2}} w_{DK}(\sigma_{i-1} \vert \sigma'_{i-2}, \sigma'_i) w_{DK} \times (\sigma_{i+1} \vert \sigma'_i, \sigma'_{i+2}) P_t(\sigma'_{i-2}, \sigma'_i, \sigma'_{i+2}). \tag{5}$$

Evidently we have an infinite hierarchy of equations. In the n-site approximation the hierarchy is truncated by estimating the $(n+1)$-site probabilities on the basis of those for n sites.

The simplest case is the one-site approximation [6,8], in which $P_t(\sigma'_{i-1}, \sigma'_{i+1})$ is factored into a product of one-site probabilities. This yields the recurrence relation

$$\rho_{t+1} = \rho_t [2p_1 - (2p_1 - p_2)\rho_t], \tag{6}$$

where $\rho_t \equiv P_t(1)$ is the density of active sites (the order parameter for the DKCA). Equation (6) admits two stationary solutions, corresponding to the possible DKCA phases: *absorbing* ($\rho = 0$), and *active*, in which, for $p_1 > 1/2$,

$$\rho = \frac{2p_1 - 1}{2p_1 - p_2}. \tag{7}$$

Thus the critical line at the site level is $p_{1c} = 1/2$.

In the pair approximation [6] the three-site probability is written in terms of the two-site quantity, using the conditional probability:

$$P_t(\sigma_{i-2}, \sigma_i, \sigma_{i+2}) \simeq \frac{P_t(\sigma_{i-2}, \sigma_i) P_t(\sigma_i \sigma_{i+2})}{P_t(\sigma_i)}. \tag{8}$$

[The one-site probabilities are given by $P_t(\sigma_i) = \Sigma_{\sigma_{i+2}} P_t(\sigma_i, \sigma_{i+2})$.] Letting $z_t \equiv P_t(1,1)$, and noting that $P_t(1,0) \equiv k_t = \rho_t - z_t$, we have the relations

$$z_{t+1} = \frac{1}{\rho_t} [p_2 z_t + p_1 k_t]^2 + p_1^2 \frac{k_t^2}{1-\rho_t} \tag{9}$$

and

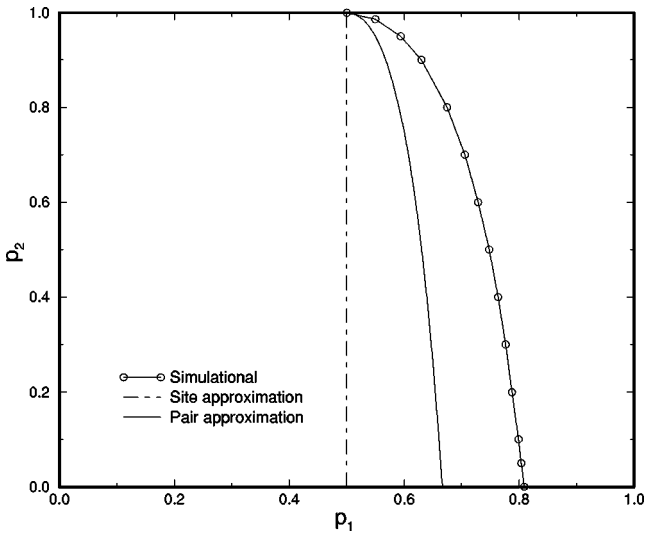

FIG. 1. DKCA phase diagram—simulation results from Ref. [21].

$$k_{t+1} = \frac{1}{\rho_t} (p_2 z_t + p_1 k_t)(q_2 z_t + q_1 k_t) + \frac{p_1 k_t}{1-\rho_t} (q_1 k_t + v_t), \tag{10}$$

where $q_i \equiv 1 - p_i$, while for $v_t \equiv P_t(0,0)$ we have

$$v_{t+1} = \frac{1}{\rho_t} [q_2 z_t + q_1 k_t]^2 + \frac{1}{1-\rho_t} [q_1 k_t + v_t]^2. \tag{11}$$

In the active stationary state, these relations imply

$$z = \frac{1-2p_1}{p_2 - 2p_1} \rho, \tag{12}$$

which leads to the stationary active-site density,

$$\rho = \frac{p_2 (p_1 - 1)^2 + p_1 (3p_1 - 2)}{(2p_1 - 1)(2p_1 - p_2)}. \tag{13}$$

In this approximation, the critical line in the (p_1, p_2) plane is

$$p_2 = \frac{p_1 (2 - 3p_1)}{(1-p_1)^2}. \tag{14}$$

The phase diagram for the DKCA in the one-and two-site approximations is compared with simulation results [21] in Fig. 1.

III. QUASISTATIONARY PROBABILITY DISTRIBUTIONS

A. Method

Since the approximations discussed in the previous section effectively consider the $L \to \infty$ limit, the densities (ρ, z, etc.), are in fact *deterministic* variables. Our goal in this paper is to construct reduced *stochastic* descriptions of a finite system, in a manner analogous to that employed in deriving n-site approximations, and to determine the associated quasistationary properties. In this section we study the problem at

the one-site level. Consider the DKCA on a ring of L sites. At the one-site level, the state of the system is specified by N_t, the number of active sites at time t. Let $p_t(N)$ $(N=0,\ldots,L)$ be the probability to have exactly N active sites at time t. The probability vector $p_t = [p_t(0), p_t(1), \ldots, p_t(L)]$, satisfies

$$p_t(N) = \sum_{N'} W(N|N') p_{t-1}(N'), \tag{15}$$

where W is the transition matrix, with $W(N|N')$ representing the probability to have N active sites at time t, given N' at time $t-1$.

At the one-site level, the state each site is treated as an independent event. Given N' active sites at time t, our best estimate for the probability x of a given site to be active at the next time step is [see Eq. (6)]

$$x = y[2p_1 - (2p_1 - p_2)y], \tag{16}$$

where $y = N'/L$. Thus the transition probabilities in the one-site approximation are

$$W(N|N') = \frac{L!}{(L-N)!N!} x^N (1-x)^{L-N}. \tag{17}$$

(Here we suppose that all configurations with the same number of active sites are equally probable, since there is no reason to prefer one such configuration over another at this level of analysis.) The one-site distribution $p_t(N)$ is therefore a superposition of binomial distributions with means $x = 0,1,\ldots,L$, the weight of a given distribution depending only on the mean population at the previous step.

Since (for L finite) the probability distribution will always evolve to the absorbing state, $p(N) = \delta_{N,0}$, it is of interest to study the quasistationary distribution $\overline{p}(N)$, defined as follows. We suppose that as $t \to \infty$, the probability distribution, *conditioned on survival*, attains a time-independent form. This means for long times

$$p_t(N) = A_t \delta_{N,0} + S_t \overline{p}(N), \tag{18}$$

where the only time dependence lies in A_t and S_t. Since the QS distribution $\overline{p}(N)$ is conditioned on survival, $\overline{p}(0) \equiv 0$. Adopting the normalization

$$\sum_{N=1}^{L} \overline{p}(N) = 1, \tag{19}$$

S_t in Eq. (18) represents the survival probability and $A_t = 1 - S_t$ the probability to have fallen into the absorbing state. The QS hypothesis is verified numerically below. Evolving the distribution in Eq. (18) to the next time step, we have

$$\begin{aligned} p_{t+1}(N) &= A_t \delta_{N,0} + S_t \sum_{N'=0}^{L} W(N|N') \overline{p}(N') \\ &= A_{t+1} \delta_{N,0} + S_{t+1} \overline{p}(N), \end{aligned} \tag{20}$$

which implies that $S_{t+1} = \alpha S_t$, where

$$\alpha = 1 - \sum_{N=1}^{L} W(0|N) \overline{p}(N). \tag{21}$$

Restricted to the states $1,\ldots,N$, $\overline{p}$ is an eigenvector of matrix W with eigenvalue α. The lifetime τ of the QS state is

$$\tau = -\frac{1}{\ln \alpha}. \tag{22}$$

One method for generating the QS distribution is via iteration of the evolution equation, Eq. (15), until the distribution $q_t(N) \equiv p_t(N)/S_t$ (for $N = 1,2,\ldots,L$), attains a time-independent form. We refer to this as the *direct* method. An alternative method [23] is based on writing the evolution in the form

$$\Delta p_t(N) \equiv p_{t+1}(N) - p_t(N) = -w(N) p_t(N) + r_t(N), \tag{23}$$

where $r_t(N) = \Sigma_{N' \neq N} W(N|N') p_t(N')$ and $w(N) = \Sigma_{N' \neq N} W(N'|N)$. Inserting the normalized QS distribution $\overline{p}(N)$ in the right-hand side (RHS) of the above relation, we have

$$(\alpha - 1)\overline{p}(N) = -w(N)\overline{p}(N) + \overline{r}(N), \tag{24}$$

where $\overline{r}(N) = \Sigma_{N'} W(N|N') \overline{p}(N')$. Noting that $1 - \alpha = \overline{r}(0)$, this may be written in the form

$$\overline{p}(N) = \frac{\overline{r}(N)}{w(N) - \overline{r}(0)}, \quad N \geqslant 1. \tag{25}$$

This relation suggests the following iterative scheme:

$$p'(N) = a p(N) + (1-a) \frac{r(N)}{w(N) - r(0)}, \tag{26}$$

where a is a parameter and $r(N)$ is evaluated using the distribution $p(N)$. At each iteration the new distribution p' must be normalized. In this way, we can construct the quasistationary state from any initial distribution $p(N)$ that is non-negative and normalized. We call this the *iterative* scheme. As discussed in Ref. [23], good convergence is obtained for $a \simeq 0$.

B. Results

We have constructed the QS distribution for the DKCA at the one-site level, using both the direct and iterative schemes. In Fig. 2 we show the time evolution of the probability distribution (conditioned on survival) at a point on the critical line. It is evident that the distribution reaches a quasistationary form after about 100 time steps. Figure 3 shows the evolution of the mean population $\langle N \rangle$, the moment ratio $m = \langle N^2 \rangle / \langle N \rangle^2$, (both conditioned on survival), and the de-

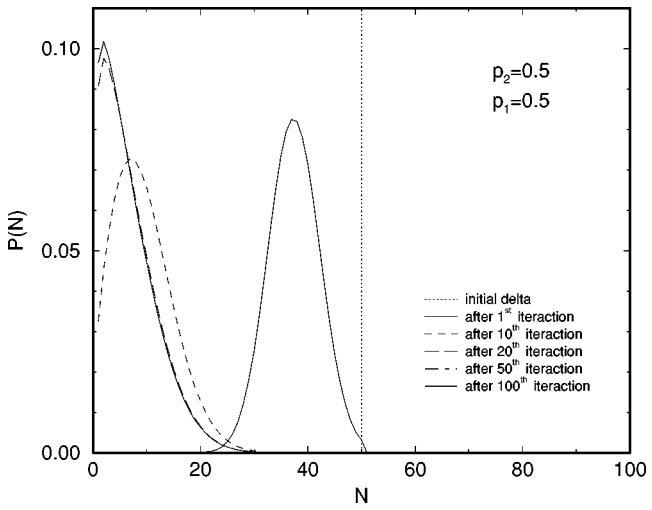

FIG. 2. Evolution of the probability distribution, conditioned on survival, in the one-site approximation. The initial distribution is $p_0(N)=\delta_{N,50}$. System size $L=100$/ $p_1=p_2=0.5$.

cay rate $\gamma=r_t(0)/S_t$, to their quasistationary values, for the same parameters as in Fig. 2. (Note that γ is the transition rate into the absorbing state.)

Relaxation to the QS state appears to consist of two stages: an initial transient, which depends strongly on the initial condition, and a long-time, exponential approach to the final values. The mean population, for example, follows $|\langle N\rangle-\langle N\rangle_{QS}|\sim e^{-t/\tau_R}$. (For the data in Fig. 3, $\tau_R\sim 9$, while the lifetime of the QS state is about 16.) We find that m and γ *relax at the same rate* as $\langle N\rangle$, and that this relaxation time is *independent of the initial distribution*. Thus the asymptotic relaxation to the QS state is governed by a relaxation time τ_R that appears to depend only on the parameters p_1 and p_2 and on the system size L.

The distribution may be further characterized by its skewness, S, and kurtosis, K, defined through the relations

$$S=\frac{\kappa_3}{\kappa_2^{3/2}} \tag{27}$$

and

$$K=\frac{\kappa_4}{\kappa_2^2}, \tag{28}$$

where κ_n is the nth cumulant of the distribution [2]. For the Gaussian distribution, both skewness and kurtosis are null ($S=K=0$). The evolution of the skewness and kurtosis is also shown in Fig. 3. Figure 4 shows the quasistationary distribution at several points in parameter space. We observe that in the frozen phase the distribution collapses to $N=1$ while in the active phase it is concentrated near $N=\langle N\rangle$.

Of particular interest are the QS scaling properties at the critical point. We have verified that $\langle N\rangle\sim L^{1/2}$ in the critical QS state. The QS lifetime scales in the same manner. These system-size dependences were encountered previously for the CP and MVP in the one-site approximation [20]. The relaxation time τ_R also grows $\sim L^{1/2}$ at the critical point; we find $\tau_{QS}/\tau_R\sim 2.67$ for $p_1=p_2=1/2$.

In the active phase, however, τ_{QS} grows $\sim\exp[\text{const.}\times(p_1-p_{1c})L]$, while τ_R varies only slightly with p_1, p_2, and L. This leads to a clear separation of time scales ($\tau_{QS}\gg\tau_R$) for large systems. (For $L=100$, $p_1=0.6$, and $p_2=0.5$, for example, $\tau_{QS}\simeq 2000$ while $\tau_R\simeq 8$.)

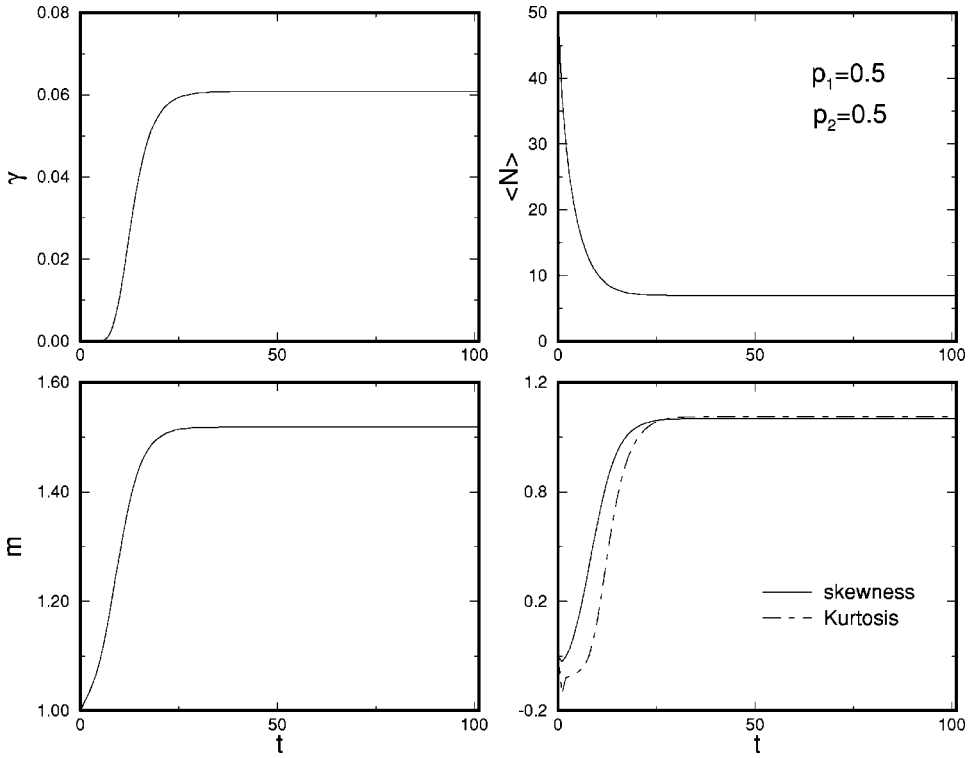

FIG. 3. Evolution toward the QS state in the one-site approximation; parameters as in Fig. 2. Upper left, decay rate γ; right, mean number of active sites. Lower left, moment ratio m; right, skewness and kurtosis.

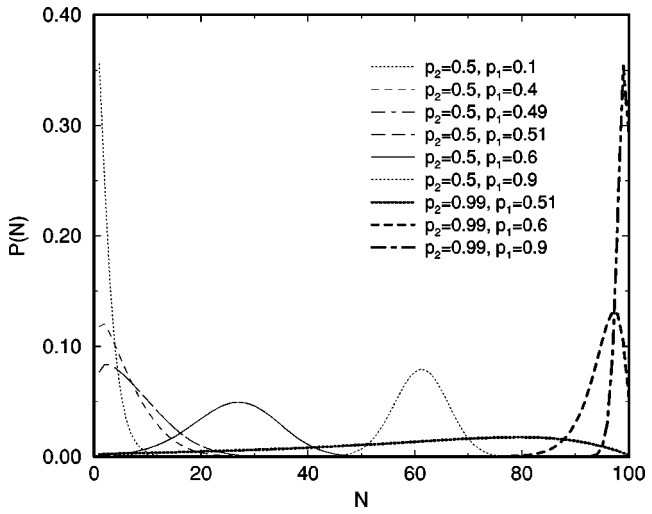

FIG. 4. QS distribution at several different points in the DKCA phase diagram, for $L=100$.

In Fig. 5 we show the QS density versus p_1 in the site approximation, for several system sizes, showing convergence to the deterministic mean-field prediction. Also shown is the moment ratio m versus p_1 for the same system sizes. Data for $L=1000-10^5$ (see Fig. 6) indicate that as $L\to\infty$ at the critical point, the moment ratio approaches the value 1.660, found for the CP in the one-site approximation, and for the Malthus-Verhulst process [20].

The moment ratio m appears to approach the same limiting value all along the critical line, for $p_2<1$. This suggests that the critical QS distribution has a scaling limit for large L, of the form

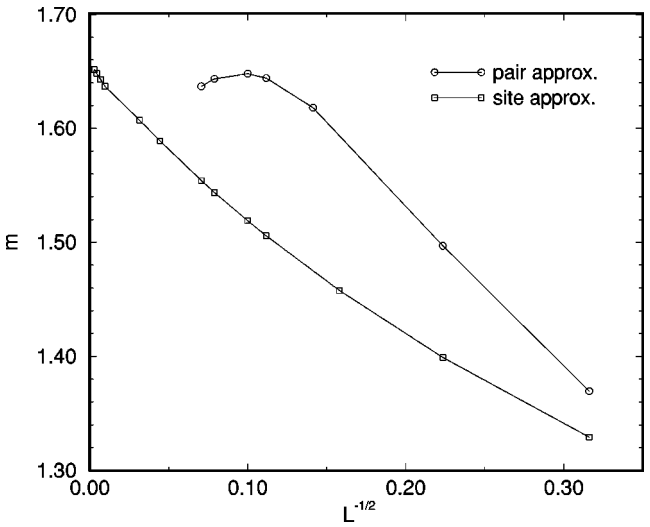

FIG. 6. Moment ratio m vs $L^{-1/2}$ at the critical point. □, one-site approximation, $p_1=p_2=1/2$; ○, pair approximation, $p_1=0.6306$, $p_2=0.5$.

$$\overline{p}(N)\simeq\frac{1}{\langle N\rangle}\mathcal{P}(N/\langle N\rangle), \tag{29}$$

where $\mathcal{P}$ is a scaling function. Figure 7 compares (for $p_1=p_2=0.5$), $\langle N\rangle\,\overline{p}(N)$ as a function of $N/\langle N\rangle$, for system sizes $L=10^3$, 10^4, and 10^5, as well as the exact scaling function for the CP and MVP found in Ref. [20]. It is interesting to note that the QS distribution for the DKCA has the same scaling form as for the CP and the MVP, despite the fact that in the critical DKCA, $\overline{p}(N)$ takes its maximum

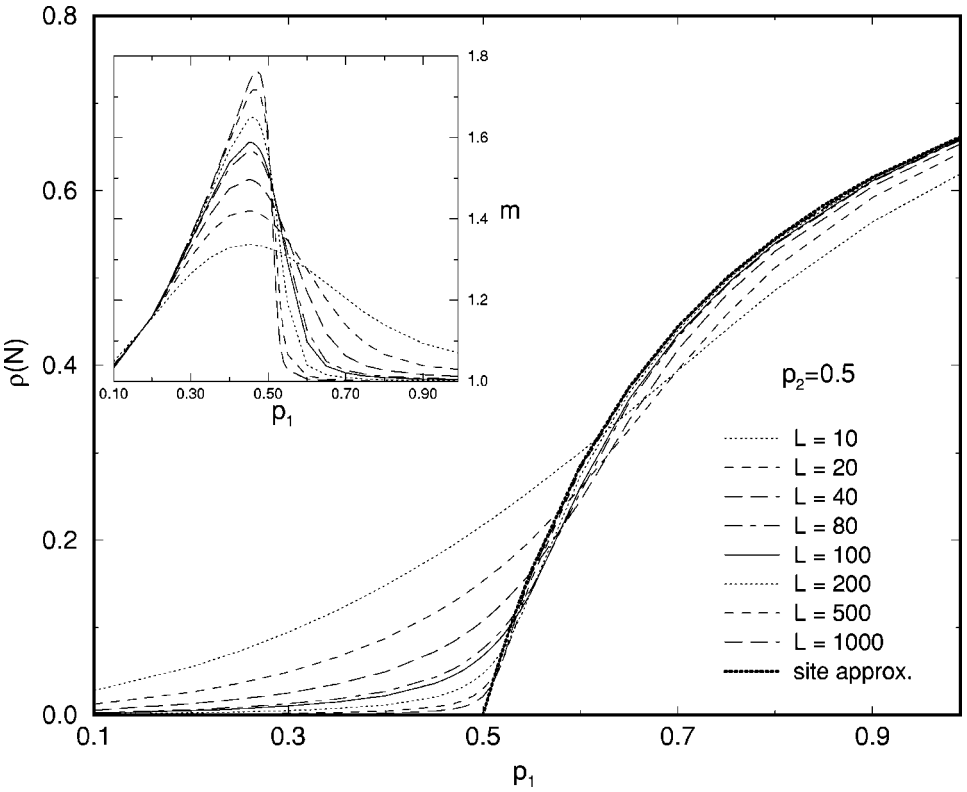

FIG. 5. Quasistationary density for the DKCA, in the site approximation, for several system sizes. The inset shows moment ratio m vs p_1 for the same system sizes.

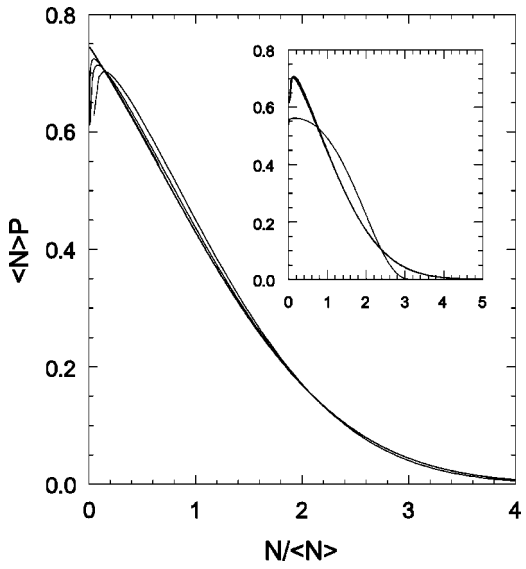

FIG. 7. Scaling plot of the QS probability distribution in the one-site approximation at the critical point ($p_1=p_2=1/2$), for $L=10^3$, 10^4, and 10^5 (curves with maxima approaching the y axis as L increases), and the asymptotic scaling function for the contact process found in Ref. [20] (with maximum at $x=0$). Inset: scaling plot of the QS distribution as in Fig. 7, for $L=2000$, $p_1=1/2$, and $p_2=0.25$, 0.5, 0.75, 0.9, and 0.999. The first four curves collapse, while the last has a broader distribution.

value for $N>1$. The position of this maximum, however, grows very slowly with L (roughly, $\sim \ln L$), so that it does not alter the infinite-size limit. A possible explanation for a maximum away from $N=1$ is that, in the DKCA, there are transitions to the absorbing state ($N=0$), from various values of N, not only for $N=1$, as is the case in the CP.

The inset of Fig. 7 shows $\langle N\rangle\ \overline{p}(N)$ versus $N/\langle N\rangle$ for $p_1=0.5$, $L=2000$, and various values of p_2. The data collapse confirms the scaling hypothesis, except for $p_2\simeq 1$. The distinct behavior in the latter case is expected, since $p_2=1$ corresponds to *compact* directed percolation, which has *two* absorbing states (all 0 or all 1). (The situation is analogous to that found in the *voter model*, a continuous-time process with two absorbing states [20].)

We find that any initial distribution not concentrated on $N=0$ evolves to the QS distribution, which is independent of the initial condition. (Uniqueness of the QS distribution is to be expected in the case of the DKCA, which has only one absorbing and one active state. A nonunique QS distribution can be envisioned for a process in which the active state exhibits symmetry breaking.)

The direct and iterative methods discussed above yield (as they must), the same QS distribution. Using a in the range -0.4 to 0, we find that the iterative method converges to the QS distribution slightly faster than the direct approach (it typically requires about 30% fewer steps). In contrast with the continuous-time case, in which the iterative method can be orders of magnitude faster than integration of the master equation [20,23], here the gain in efficiency is quite modest. This is not surprising, since the enormous gain in efficiency for continuous-time processes is associated with the small time step required to maintain numerical stability, in the usual direct integration schemes. In the present case, the direct method has an effective time step of unity.

TABLE II. Allowed values for Z on a ring.

N	Z
0,1	0
$2,\ldots,L/2$	$0,\ldots,N-1$
$L/2,\ldots L-1$	$2N-L,\ldots,N-1$
L	L

IV. PAIR APPROXIMATION

A. Method

In this section we construct the quasistationary probability distribution for the DKCA at the pair level. The system is described by two stochastic variables, the number of occupied sites N, and the number of doubly occupied nearest-neighbor (NN) pairs, Z. We consider a ring of L sites. [For convenience we introduce a different notation for the site variables, defining $\varphi_i=\sigma_{i/2}$ for even t and $\varphi_i=\sigma_{(i+1)/2}$ for odd t. In this way the site index always takes the values $1,\ldots,L$ at all times, and NN sites have state variables φ_i and φ_{i+1}.]

To begin, we establish the allowed range of values for Z. Using "1" and "0" to represent occupied and vacant sites, respectively, we denote by K the number of (10) NN pairs. [By symmetry, the number of (01) pairs is also K.] K is not an independent variable, since each 1 is followed by a 0 or another 1, yielding $N=Z+K$. Similarly, the number of (00) pairs, V, is given by $V=L-2N+Z$. The conditions $K\geqslant 0$ and $V\geqslant 0$ imply certain limits for Z on a ring of L sites, listed in Table II.

Next we construct the transition probabilities $W(N,Z|N',Z')$. Note that the presence of V' (00) pairs at time t implies that there are at least this many vacant *sites* at time $t+1$; thus $W=0$ for $N>2N'-Z'$. We proceed by analogy with the one-site approximation: given N' and Z', we first determine the *pair densities* $z=Z/L$, k, and v using Eqs. (9)–(11). (Here z, k, and v represent the densities at time $t+1$, while the variables appearing on the RHS of each equation are evaluated using $\rho_t=N'/L$ and $z_t=Z'/L$.) We treat all configurations having the same N and Z as equally probable, and estimate the probability of any one such configuration as

$$Q(N,Z;\rho,z)\equiv\left[\frac{z^Z k^{2K} v^V}{\rho^N(1-\rho)^{L-N}}\right]\frac{1}{L}\sum_{j=1}^{L}\frac{s_j s_{j+1}}{p_j}, \qquad (30)$$

where $k=\rho+z$. The first factor (in square brackets) is the product of all pair probabilities, divided by the product of all site probabilities. The second factor represents a correction, needed for normalization of Q, which arises as follows. Suppose we construct the probability Q starting at site j, so that the first factor in the product is p_j, i.e., the pair probability associated with sites j and $j+1$. The next factor will then be

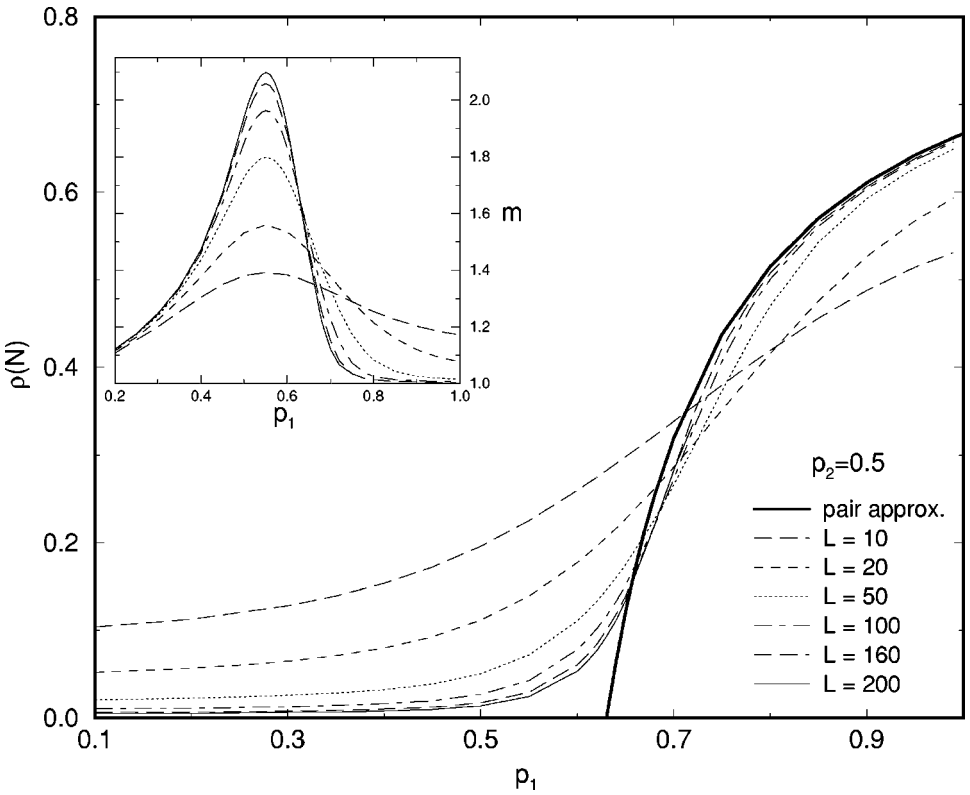

FIG. 8. Quasistationary active-site density versus p_1 for the DKCA in the pair approximation, for several system sizes. The inset shows the moment ratio m for the same system sizes.

p_{j+1}/s_{j+1}, which represents the conditional probability of the variable at site $j+2$, given the state of site $j+1$, and so on. When we close the ring, adding the link between sites $j-1$ and j, the final factor is $P(\varphi_{j-1},\varphi_j|\varphi_{j-1},\varphi_j)=1$, *not* $P(\varphi_{j-1},\varphi_j)/[P(\varphi_{j-1})P(\varphi_j)]$. So the first factor in Eq. (30) has one pair factor, and two site factors, too many, and should be multiplied by $s_{j-1}s_j/p_{j-1}$. Since the position of the starting link is arbitrary, we take the mean of this correction over the ring.

Note that the correction factor may be written as

$$\frac{1}{L}\sum_{j=1}^{L}\frac{s_j s_{j+1}}{p_j}=\frac{1}{L}\left[Z\frac{\rho^2}{z}+2K\frac{\rho(1-\rho)}{k}+V\frac{(1-\rho)^2}{v}\right]. \tag{31}$$

In case the pair numbers take their *expected values* ($Z=Lz$, etc.), the correction factor is unity.

The transition probability is the product of a configurational probability $Q(N,Z;\rho,z)$ and the number of configurations, $\Gamma(N,Z;L)$, having exactly N active sites and Z active pairs on a ring of L sites:

$$W(N,Z|N',Z')=\Gamma(N,Z;L)Q(N,Z;\rho,z), \tag{32}$$

for $(N,Z)\neq(N',Z')$ and $N\leqslant 2N'-Z'$; for $N>2N'-Z'$, $W=0$; if $(N,Z)=(N',Z')$,

$$W(N',Z'|N',Z')=1-\sum_{N,Z}{}^{*}\ \Gamma(N,Z;L)Q(N,Z;\rho,z), \tag{33}$$

where (*) denotes the exclusion of the single term $N=N'$, $Z=Z'$. An expression for the combinatorial factor $\Gamma(N,Z;L)$ is derived in the Appendix. (Note that $\Gamma=0$ for values of N and Z outside the permitted range given in Table II.) The evolution of the probability distribution follows:

$$p_{t+1}(N,Z)=\sum_{N',Z'|2N'-Z'\geqslant N}W(N,Z|N',Z')p_t(N',Z'). \tag{34}$$

B. Results

We constructed the QS distribution at the pair level for the DKCA, for systems of up to 200 sites, focusing on the behavior in the vicinity of the critical line. (The computation is considerably more demanding of memory and cpu time than is the one-site approximation; the chief limitation is the evaluation of the coefficients Γ.)

Figure 8 shows the QS order parameter versus p_1 in the pair approximation, for several system sizes. We also plot the moment ratio m, showing a series of crossings whose location approaches the critical point as $L\to\infty$. The behavior of m versus L, at criticality, is shown in Fig. 6. In Fig. 9 we show the QS distribution, $\overline{p}(N,Z)$, at criticality ($p_2=0.5$, $p_1=0.6306$), for $L=100$. The marginal distribution $\overline{p}(N)$ is similar to that found in the site approximation. The behavior of the mean population, moment ratio, decay rate, skewness and kurtosis, as functions of time, is again qualitatively similar to that observed in the site approximation.

V. DISCUSSION

We studied the quasistationary properties of the DKCA in the one- and two-site approximations. Our study represents

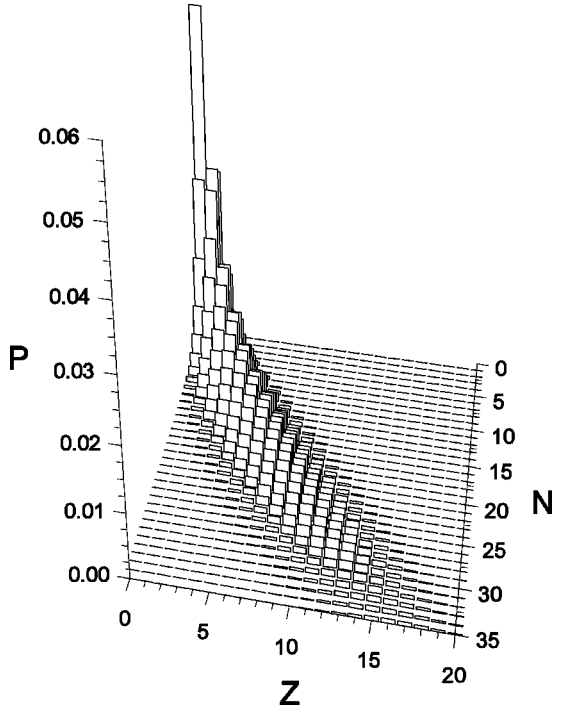

FIG. 9. QS pair density probability distribution, conditioned on survival, at criticality ($p_2=0.5$, $p_1=0.6306$).

an extension of QS analysis, applied to continuous-time models exhibiting an absorbing-state phase transition in Ref. [20], to discrete-time processes.

Compared with continuous-time processes, the numerical analysis of a discrete-time system is simpler, since it involves iteration rather than integration of a set of differential equations. While this is evident at the one-site level, at higher levels of approximation the advantage is tempered by the fact that starting from a given configuration, transitions to many (or all) other configurations are possible. The resulting need for combinatorial factors [e.g., $\Gamma(N,Z;L)$] complicates the analysis.

An interesting result of our study is that the scaling behavior along the critical line is the same for the continuous-time contact process (and the closely related Malthus-Verhulst process) as for the discrete-time DKCA. In particular, the QS order parameter decreases $\sim 1/\sqrt{L}$ in both cases, while the QS lifetime grows $\sim \sqrt{L}$. While the universality of global scaling could have been anticipated on the basis of the central limit theorem, the similarity extends further, to include the detailed form of the scaling function governing the QS probability distribution and its associated moments. Thus the situation is analogous to that found numerically in studies of absorbing-state phase transitions: not only critical exponents, but moment ratios of the order parameter take universal values at the critical point [24].

ACKNOWLEDGMENT

This work was financially supported by CNPq, Brazil.

APPENDIX

To evaluate $\Gamma(N,Z;L)$, the number of configurations on a ring of L sites with exactly N active sites and Z nearest-neighbor pairs of active sites, we observe that the associated generating function $\zeta(x,y;L)=\Sigma_{N,Z}\Gamma(N,Z;L)x^Z y^N$, can be written as the partition function for a one-dimensional lattice gas:

$$\zeta(x,y;L)=\sum_{\sigma_1=0}^{1}\cdots\sum_{\sigma_L=0}^{1} x^{\sum_i \sigma_i\sigma_{i+1}}\, y^{\sum_i \sigma_i}, \qquad \text{(A1)}$$

with $\sigma_{N+1}\equiv\sigma_1$. (We note in passing that $x=e^{\beta J}$ and $y=e^{\beta\mu}$ for the lattice gas with nearest-neighbor interaction J, chemical potential μ, and inverse temperature β.) The partition function is evaluated using the transfer matrix $T(\sigma,\sigma')=x^{\sigma\sigma'}y^{(\sigma+\sigma')/2}$:

$$\zeta(x,y;L)=\mathrm{Tr}T^L \qquad \text{(A2)}$$

$$=\lambda_1^L+\lambda_2^L, \qquad \text{(A3)}$$

where $\lambda_{1,2}$ are the eigenvalues of T:

$$\lambda_{1,2}=1/2(1+xy\pm\sqrt{(1-xy)^2+4y}). \qquad \text{(A4)}$$

For L even, we have

$$(a+b)^L+(a-b)^L=2\sum_{n=0}^{L/2}\binom{L}{2n}a^{2n}b^{L-2n}, \qquad \text{(A5)}$$

so that

$$\lambda_1^L+\lambda_2^L=2\sum_{n=0}^{L/2}\binom{L}{2n}\left(\frac{1+xy}{2}\right)^{2n}\left(\frac{(1-xy)^2+4y}{4}\right)^{L/2-n}, \qquad \text{(A6)}$$

leading to

$$\lambda_1^L+\lambda_2^L=2y^{L/2}\sum_{n=0}^{L/2}\sum_{m=0}^{2n}\sum_{p=0}^{L/2-n}\sum_{q=0}^{2p}\binom{L}{2n}\binom{2n}{m}\times\binom{\frac{L}{2}-n}{p}\binom{2p}{q}\frac{(-1)^q(xy)^{m+q}}{(4y)^{n+p}}. \qquad \text{(A7)}$$

The coefficient of $x^Z y^N$ is

$$\Gamma(N,Z;L)=\frac{2}{4^{L/2+Z-N}}\sum_{n=0}^{L/2}\sum_{m=0}^{2n}\binom{L}{2n}\binom{2n}{m}\binom{\frac{L}{2}-n}{\frac{L}{2}-n+Z-N}\times\binom{L+2(Z-N-n)}{Z-m}(-1)^{Z-m}. \qquad \text{(A8)}$$

The above expression is evaluated numerically.

[1] E. Domany and W. Kinzel, Phys. Rev. Lett. **53**, 311 (1984).
[2] N.G. van Kampen, *Stochastic Processes in Physics and Chemistry* (North-Holland, Amsterdam, 1992).
[3] R. Dickman, M.A. Muñoz, A. Vespignani, and S. Zapperi, Braz. J. Phys. **30**, 27 (2000).
[4] J. Marro and R. Dickman, *Nonequilibrium Phase Transitions in Lattice Models* (Cambridge University Press, Cambridge, England, 1999).
[5] H. Hinrichsen, Adv. Phys. **49**, 815 (2000).
[6] T. Tomé, Physica A **212**, 99 (1994).
[7] F. Bagnoli, N. Boccara, and R. Rechtman, Phys. Rev. E **63**, 046116 (2001).
[8] H.A. Gutowitz, J.D. Victor, and B.W. Knight, Physica D **28**, 18 (1987).
[9] W. Kinzel, Z. Phys. B: Condens. Matter **58**, 229 (1985).
[10] M.L. Martins, H.F. Verona de Resende, C. Tsallis, and A.C.N. deMagalhães, Phys. Rev. Lett. **66**, 2045 (1991).
[11] G.A. Kohring and M. Schreckenberg, J. Phys. I **2**, 2033 (1992).
[12] H. Hinrichsen, J.S. Weitz, and E. Domany, J. Stat. Phys. **88**, 617 (1997).
[13] A.P.F. Atman and J.G. Moreira, Eur. Phys. J. B **16**, 501 (2000).
[14] T. Tomé and M.J. de Oliveira, Phys. Rev. E **55**, 4000 (1997).
[15] F. Bagnoli, R. Bulajich, R. Livi, and A. Maritan, J. Phys. A **25**, L1071 (1992).
[16] A. Kemper, A. Schadschneider, and J. Zittarz, J. Phys. A **34**, 7769 (2001).
[17] A.M. Yaglom, Dokl. Akad. Nauk SSSR **56**, 797 (1947).
[18] P.A. Ferrari, H. Kesten, A. Martínez, and P. Picco, Ann. Prob. **23**, 501 (1995); P.A. Ferrari, H. Kesten, and A. Martínez, Ann. Appl. Probab. **6**, 577 (1996).
[19] I. Nasell, Math. Biosci. **107**, 187 (1991).
[20] R. Dickman and R. Vidigal, J. Phys. A **35**, 1147 (2002).
[21] A.P.F. Atman, R. Dickman, and J.G. Moreira, Phys. Rev. E **66**, 016113 (2002); e-print cond-mat/0109441.
[22] T. Tomé and M. J. de Oliveira, *Dinâmica Estocástica e Probabilidade* (Edusp, São Paulo, 2001).
[23] R. Dickman, Phys. Rev. E **65**, 047701 (2002).
[24] R. Dickman and J. Kamphorst Leal da Silva, Phys. Rev. E **58**, 4266 (1998).